

$X(3872)$ electromagnetic decay in a coupled-channel model*

MARCO CARDOSO

CFTP, Instituto Superior Técnico, Universidade de Lisboa, Lisbon, Portugal

GEORGE RUPP

CFIF, Instituto Superior Técnico, Universidade de Lisboa, Lisbon, Portugal

EEF VAN BEVEREN

CFC, Departamento de Física, Universidade de Coimbra, Coimbra, Portugal

A multichannel Schrödinger equation with both quark-antiquark and meson-meson components, using a harmonic-oscillator potential for $q\bar{q}$ confinement and a delta-shell string-breaking potential for decay, is applied to the axial-vector $X(3872)$ and lowest vector charmonia. The model parameters are fitted to the experimental values of the masses of the $X(3872)$, J/ψ and $\psi(2S)$. The wave functions of these states are computed and then used to calculate the electromagnetic decay widths of the $X(3872)$ into $J/\psi\gamma$ and $\psi(2S)\gamma$.

PACS numbers: 12.39.Pn, 12.40.Yx, 13.20.Gd, 13.40.Hq

1. Introduction

The $X(3872)$ was discovered in 2003 by the Belle Collaboration [1], and later confirmed in CDF [2] and D0 [3] experiments. Its PDG[4] mass and width are now $M_X = 3871.69 \pm 0.17 \text{ MeV}$ and $\Gamma_X < 1.2 \text{ MeV}$, respectively. According to experiment it has quantum numbers $J^{PC} = 1^{++}$ [5] and $I^G = 0^+$ [6, 7]. The $X(3872)$ seems to be difficult to describe as a simple $c\bar{c}$ state.

Its main decays are into $\rho^0 J/\psi$, $\omega J/\psi$ and $DD\pi$, with the latter final state resulting mainly from an intermediate DD^* channel. The first two channels are OZI forbidden and the decay into $\rho^0 J/\psi$ also violates isospin

* Presented by M. Cardoso at the Workshop “EEF70”, Coimbra, Portugal, September 1–5, 2014

Collaboration	\mathcal{R}_ψ
Belle [9]	< 2.1
BaBar [10]	3.4 ± 1.4
LHCb [11]	$2.46 \pm 0.64 \pm 0.29$

Table 1. Measured values of the EM rate ratio \mathcal{R}_ψ .

conservation. Both are therefore highly suppressed. As the mass is below the DD^* thresholds ($E_{D^0 D^{0*}} = 3871.84$ MeV and $E_{D^\pm D^{\mp*}} = 3879.90$ MeV), which are the lowest OZI-allowed decay channels, the $X(3872)$ can be seen as a quasi-bound state.

Here we will study the $X(3872)$ as a unitarized mesonic state, that is, one with both quark-antiquark and meson-meson (MM) components. A previous configuration-space calculation [8] with $c\bar{c}$ and $D^0 D^{0*}$ components predicted a state with approximately 7.5% $c\bar{c}$. We now generalize that calculation to include other possible channels.

Electromagnetic (EM) decays of the $X(3872)$ were observed by Belle [9], Babar [10] and LHCb [11]. Babar and LHCb observed decays into $J/\psi\gamma$ and $\psi(2S)\gamma$, and found the ratio of partial decay widths

$$\mathcal{R}_\psi = \frac{\Gamma(\psi(2S)\gamma)}{\Gamma(J/\psi\gamma)}$$

to be of the order of 2.5–3.5, whereas Belle did not observe the decay into $\psi(2S)\gamma$ at all and set an upper limit on the value of \mathcal{R}_ψ (see Table 1).

2. Method

We first derive the wave functions of J/ψ , $\psi(2S)$ and $X(3872)$, considering all $c\bar{c}$, DD (only for vector charmonia), DD^* and D^*D^* channels, where $D^{(*)}$ is shorthand for $D^{(*)0}$, $D^{(*)\pm}$, or $D_s^{(*)\pm}$. With these, the EM transition matrix elements and resulting decay widths will be calculated.

In the present model, a unitarized meson is not just a $q\bar{q}$ state but it also has MM components:

$$|\psi\rangle = \sum_c |\psi_{q\bar{q}}^c\rangle + \sum_j |\psi_{MM}^j\rangle. \quad (2.1)$$

In the quark-antiquark sector we have confinement realized through a harmonic-oscillator (HO) potential with universal (i.e., mass-independent) frequency:

$$V_{Q\bar{Q}}(r) = \frac{1}{2}\mu_c\omega^2 r^2. \quad (2.2)$$

As for the MM sector, we assume no direct interactions and only a string-breaking potential that links the $q\bar{q}$ and MM channels to one another:

$$V_{cj} = \frac{\lambda g_{cj}}{2\mu_c} \delta(r - a) . \quad (2.3)$$

We take the parameters $m_c = 1.562 \text{ GeV}$ and $\omega = 0.190 \text{ GeV}$ unchanged with respect to all our previous work. In the 1^{--} and 1^{++} cases, somewhat different values of the overall coupling λ will be applied, viz. λ_ψ and λ_X , respectively, to be determined from the physical charmonium masses. Furthermore, the J/ψ and $\psi(2S)$ masses will also be used to fix the value of the string-breaking distance a , which we will take the same for the $X(3872)$. Finally, the g_{cj} are 3P_0 coupling coefficients.

Next we solve the coupled-channel Schrödinger equation

$$\begin{bmatrix} \hat{h}_{q\bar{q}}^c & V_{cj} \\ V_{jc}^\dagger & \hat{h}_{MM}^j \end{bmatrix} \begin{bmatrix} u_c \\ v_j \end{bmatrix} = E \begin{bmatrix} u_c \\ v_j \end{bmatrix} , \quad (2.4)$$

with

$$\begin{aligned} \hat{h}_{q\bar{q}}^c &= m_q^c + m_{\bar{q}}^c + \frac{\hbar^2}{2\mu_c} \left(-\frac{d^2}{dr^2} + \frac{l_c(l_c + 1)}{r^2} \right) + \frac{1}{2}\mu_c\omega^2 r^2 , \\ \hat{h}_{MM}^j &= M_1^j + M_2^j + \frac{\hbar^2}{2\mu_j} \left(-\frac{d^2}{dr^2} + \frac{L_j(L_j + 1)}{r^2} \right) . \end{aligned}$$

The solutions are known for $r \neq a$ and appropriate boundary conditions:

$$u_c(r) = \begin{cases} a_c M(-\nu_c, l_c + \frac{3}{2}, \mu_c \omega r^2) e^{-\frac{1}{2}\mu_c \omega r^2} r^{1+l_c} , & r < a , \\ b_c U(-\nu_c, l_c + \frac{3}{2}, \mu_c \omega r^2) e^{-\frac{1}{2}\mu_c \omega r^2} r^{1+l_c} , & r > a , \end{cases} \quad (2.5)$$

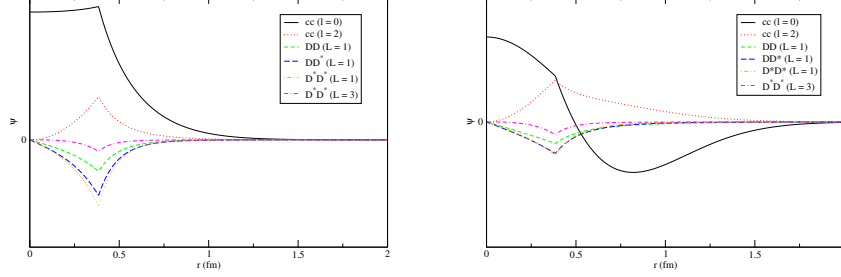
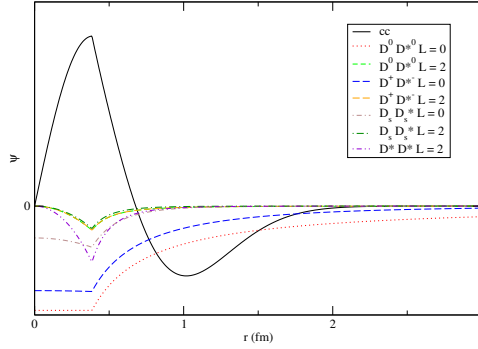
and

$$v_j(r) = \begin{cases} A_j i_{L_j}(q_j r) r , & r < a , \\ B_j k_{L_j}(q_j r) r , & r > a . \end{cases} \quad (2.6)$$

Using now continuity of the wave function and discontinuity of its derivative, we can solve the equations for a_c , b_c , A_j and B_j . The value of the energy E (for fixed λ) or coupling λ (for fixed E) is then given by the equation ($\alpha_c \equiv a_c M_c$)

$$\left(\frac{U'_c}{U_c} - \frac{M'_c}{M_c} \right) \alpha_c = \lambda^2 \sum_{jd} \frac{\mu_j g_{cj}}{2\mu_c \omega q_j a^3} \left(\frac{k'_j}{k_j} - \frac{i'_j}{i_j} \right)^{-1} \frac{e^{\frac{1}{2}(\mu_c - \mu_d)\omega a^2} g_{dj}}{\mu_d} \alpha_d . \quad (2.7)$$

For more details, see [12].

Fig. 3.1. Wave-function components of the J/ψ and $\psi(2S)$ Fig. 3.2. Wave-function components of the $X(3872)$

3. Wave functions

Using the method outlined in Sec. 2, and fitting λ_ψ as well as a to the experimental J/ψ and $\psi(2S)$ masses, we find $\lambda_\psi = 2.53$ and $a = 1.95 \text{ GeV}^{-1}$. The resulting wave-function components are plotted in Fig. 3.1. Next we adjust λ_X to the $X(3872)$ mass while keeping a the same, which yields the wave-function components shown in Fig. 3.2. The three wave-function compositions are given in Table 2. We see that the J/ψ and $\psi(2S)$ are mostly $c\bar{c}$ states, whereas the $X(3872)$ has a dominant $D^0 D^{*0}$ component. Still, its $c\bar{c}$ probability of 26.8% is a huge increase as compared to the 7.5% in [8].

	$c\bar{c}$	DD	$D^0 D^{*0}$	$D^\pm D^{*\mp}$	$D^* D^*$
J/ψ	83.6%	2.1%	6.0%	8.3%	
$\psi(2S)$	94.5%	1.3%	2.1%	2.1%	
$X(3872)$	26.8%	-	65.0%	7.0%	1.2%

Table 2. Compositions of the three charmonia ($D^{(*)}$: shorthand, see text.)

4. Electromagnetic decay

To compute the EM decay widths we use the Fermi golden rule

$$\Gamma_{i \rightarrow f} = \frac{2\pi}{\hbar} |\langle \Psi_f | \hat{H}_{int} | \Psi_i \rangle|^2 \rho_f, \quad (4.1)$$

with density of states $\rho_f = \frac{1}{2\pi\hbar c}$ [13]. To evaluate the matrix elements in 4.1, we note that the initial and final states are given by $|\Psi_i\rangle = |\psi_{nJM}\rangle \otimes |0\rangle$ and $|\Psi_f\rangle = |\psi_{n'J'M'}\rangle \otimes |\gamma_{\lambda klm}\rangle$, where l and m are the angular-momentum quantum numbers, and λ the polarization.

Expanding the wave function, we get a matrix element

$$\langle \Psi_f | \hat{H}_{int} | \Psi_i \rangle = \sum_{cc'} \langle \psi_{q\bar{q}}^c | \hat{h}_{int}^{cc'} | \psi_{q\bar{q}}^{c'} \rangle + \sum_{jj'} \langle \psi_{MM}^j | \hat{h}_{int}^{jj'} | \psi_{MM}^{j'} \rangle, \quad (4.2)$$

as we only consider transitions of the types $(Q\bar{Q})^* \rightarrow Q\bar{Q} + \gamma$ and $(M_1 M_2)^* \rightarrow M_1 M_2 + \gamma$, neglecting those like $M_1^* M_2^* \rightarrow M_1 M_2 + \gamma$.

The interaction Hamiltonian \hat{h}_{int} is obtained from minimal coupling, accounting for a possible anomalous magnetic moment. In the radiation gauge $\nabla \cdot \mathbf{A} = 0$ and $A^0 = 0$, and neglecting the \mathbf{A}^2 term, we have

$$\hat{h}_{int} = \sum_i \frac{iQ_i}{m_i c} \mathbf{A}(\mathbf{x}_i) \cdot \nabla_i - \mu_i \mathbf{S}_i \cdot \mathbf{B}(\mathbf{x}_i). \quad (4.3)$$

The EM vector potential is expanded as

$$\mathbf{A}(\mathbf{r}, t) = \sqrt{4\pi\hbar c} \sum_{\lambda lm} \int \frac{dk}{2\pi} \frac{1}{\sqrt{2\omega_k}} [\mathbf{f}_{klm}^{(\lambda)}(\mathbf{r}) e^{-i\omega_k t} a_{\lambda lm}(k) + h.c.],$$

with $a_{\lambda lm}$ being photon-annihilation operators. Components with $\lambda = e$ correspond to electric multipole radiation and the ones with $\lambda = m$ to magnetic multipole radiation. For the same l , they have opposite parity.

The $X(3872)$ (1^{++} state) can only decay into J/ψ and $\psi(2S)$ (1^{--} states) by emitting electric-dipole ($l = 1$) or magnetic-quadrupole ($l = 2$) photons.

The computation of the matrix elements is carried out as in [13]. The resulting EM decay widths are presented in Table 3. We obtain an EM rate ratio $\mathcal{R}_\psi = 1.17$.

5. Conclusions

We have generalized a previous configuration-space calculation [8] of the $X(3872)$ by including more MM channels. Thus we obtained an increase

	Complete	$c\bar{c}$	MM	Quenched
$\Gamma_e(X \rightarrow J/\psi\gamma)$	24.2	14.9	1.11	0.48
$\Gamma_m(X \rightarrow J\psi\gamma)$	0.44	0.34	0.01	0.14
$\Gamma_e(X \rightarrow \psi'\gamma)$	28.8	28.0	0.01	158
$\Gamma_m(X \rightarrow \psi'\gamma)$	0.07	0.07	0.00	0.26

Table 3. Computed EM decay widths in keV. The second and third columns show the hypothetical widths from the $c\bar{c}$ and MM components only. The last column gives the predictions of an HO quenched quark model, with the same m_c and ω as in the unquenched case. Note that these numbers are slightly different from those presented at the workshop, after correction of minor numerical errors.

of the total $c\bar{c}$ probability from 7.5% to 26.8%. This seemingly paradoxical result has a simple explanation: the inclusion of more MM channels leads to a reduction of the $D^0 D^{*0}$ component, which — due to its long tail — was responsible for an MM probability exceeding 90% [8]. Table 3 shows that unquenching very strongly affects the EM widths. Our prediction of the ratio $\mathcal{R}_\psi = 1.17$ is consistent with the result of Belle, but does not fully agree with BaBar and LHCb. However, there is an enormous improvement when compared to a quenched HO calculation. For a more detailed discussion, see [12].

M. Cardoso was supported by FCT, contract SFRH/BPD/73140/2010.

REFERENCES

- [1] S.-K. Choi *et al.* [Belle Collaboration], *Phys. Rev. Lett.* **91**, 262001 (2003).
- [2] D. Acosta *et al.* [CDF Collaboration], *Phys. Rev. Lett.* **93**, 072001 (2004).
- [3] V. M. Abazov *et al.* [D0 Collaboration], *Phys. Rev. Lett.* **93**, 162002 (2004).
- [4] K. A. Olive *et al.* [Particle Data Group Collaboration], *Chin. Phys.* **C38**, 090001 (2014).
- [5] R. Aaij *et al.* [LHCb Collaboration], *Phys. Rev. Lett.* **110**, 222001 (2013).
- [6] B. Aubert *et al.* [BaBar Collaboration], *Phys. Rev.* **D71**, 031501 (2005).
- [7] S.-K. Choi *et al.* [Belle Collaboration], *Phys. Rev.* **D84**, 052004 (2011).
- [8] S. Coito, G. Rupp, E. van Beveren, *Eur. Phys. J.* **C73**, 2351 (2013).
- [9] V. Bhardwaj *et al.* [Belle Collaboration], *Phys. Rev. Lett.* **107**, 091803 (2011).
- [10] B. Aubert *et al.* [BaBar Collaboration], *Phys. Rev. Lett.* **102**, 132001 (2009).
- [11] R. Aaij *et al.* [LHCb Collaboration], *Nucl. Phys.* **B886**, 665 (2014).
- [12] M. Cardoso, G. Rupp, E. van Beveren, arXiv:1411.1654v2 [hep-ph], accepted for publication in *Eur. Phys. J. C*.
- [13] A. G. M. Verschuren, C. Dullemond, E. van Beveren, *Phys. Rev.* **D44**, 2803 (1991).